

Numerical Investigations of Co-Flow Jet Airfoil with and without Suction

Ge-Cheng Zha,* Wei Gao,† Craig D. Paxton ‡ Alexis Palewicz§
Dept. of Mechanical and Aerospace Engineering
University of Miami
Coral Gables, Florida 33124
E-mail: gzha@miami.edu

Abstract

The airfoil with injection only is compared with the CFJ airfoil with both injection and suction with the similar injection momentum coefficient. The CFD simulations indicate that the suction of the CFJ airfoil significantly enhances the mixing and energy transfer between the jet and main flow, which results in higher circulation, higher lift, higher stall angle of attack, lower drag, and lower energy expenditure. The equivalent drag of the airfoil with injection only is significantly higher than the drag of the CFJ airfoil with both injection and suction. Since any airfoil with a jet injection needs to have a jet suction to satisfy the mass conservation law, this study indicates that the suction occurring on the suction surface such as the CFJ airfoil is more beneficial than drawing the jet mass flow from the aircraft engine inlet.

* Associate Professor

† Graduate Student

‡ Graduate Student, Current address: Boeing Company, Phantom Works, Huntsville, AL

§ Undergraduate Student

1 Nomenclature

A	Area
AoA	Angle of Attack
CFD	Computational Fluid Dynamics
CFJ	Co-Flow Jet
CC	Circulation Control
C_L	Lift Coefficient
C_D	drag Coefficient
C_μ	Momentum Coefficient
D	Drag
E	Endurance
F	Resultant Force
FC	Flow Control
\dot{m}	Mass Flow Rate
k	Turbulent Kinetic Energy
L	Lift
M	Mach Number
p	Static pressure
P	Power required
P_t	Total Pressure
R	Force from airfoil surface integral
R'	Reaction force of R
Re	Reynolds number
S	Wing Span Area ($b \times chord$)
u,v,w	Velocity components in x-, y-, and z-direction
V	Velocity vector
y^+	non-dimensional length scale for turbulent boundary layer

Subscripts:

e	control volume exit
ei	engine inlet
j	jet injection
∞	Freestream

Greek Letters:

ϵ	Turbulent Dissipation Rate
γ	Ratio of Specific Heats
ρ	Density
∞	Freestream
α	Angle of Attack
θ	Angle between slot surface and the line normal to chord

2 Introduction

Flow control (FC) is a promising means to significantly improve airfoil performance and has attracted more and more attention lately as the technology for future high performance high efficiency

aircraft[1, 2, 3, 4, 5, 6, 7]. Zha el al. have recently developed a new airfoil flow control technique using co-flow jet [8, 9, 10, 11], which dramatically increases lift, stall margin, and drag reduction.

The co-flow jet airfoil is to open an injection slot near leading edge and a suction slot near trailing edge on the airfoil suction surface. A high energy jet is injected near leading edge tangentially and the same amount of mass flow is sucked in near trailing edge. The turbulent shear layer between the main flow and the jet causes strong turbulence diffusion and mixing under severe adverse pressure gradient, which enhances lateral transport of energy from the jet to mainflow and allows the main flow to overcome severe adverse pressure gradient and remain attached at high angle of attack(AoA). The high energy jet induces high circulation and hence generates high lift. The energized main flow fills the wake and therefore reduce drag. The CFJ airfoil can recirculate the jet mass flow to achieve zero net jet mass flow and minimize the penalty to propulsion system due to no dumped jet mass flow.

In [8, 9, 11], an overview of different flow control methods is given. Compared with the circulation control (CC) airfoil[12, 13], the working mechanism of CFJ airfoil is different. A CC airfoil relies on large leading edge(LE) or trailing edge (TE) to have the Coanda effect and enhance circulation. The large TE or LE hence are required, which may generate large drag during cruise. The CFJ airfoil relies on the wall jet mixing with the main flow to energize the main flow and overcome the adverse pressure gradient so that the flow can induce high circulation and remain attached at high AoA. The CC airfoil dumps away the jet mass flow, which is a considerable penalty to the propulsion system. The CFJ airfoil recirculates the jet mass flow and achieves the zero net jet mass flow to significantly reduce the penalty to propulsion system. A CC airfoil without LE injection will reduce stall margin even though it increase the lift[14]. Compared with the synthetic jet flow control, the enhancement of airfoil performance by the CFJ airfoil is much more dramatic because the interaction of the synthetic jet with the main flow is weak[8, 9, 15]. The synthetic jet airfoil also has little stall margin increase[15]. CFJ airfoil simultaneously achieves three dramatic effects at low energy expenditure: lift enhancement, stall margin increase, and drag reduction. The mission analysis conducted in [8] indicates a significant improvement of fuel consumption reduction, increase of range and endurance, and a dramatic reduction of take off and landing distance.

The turbulent mixing between the jet and main flow to transfer energy from the jet to the main flow is the fundamental working principle of CFJ airfoil [8, 11]. The CFJ airfoil performance is more sensitive to the injection than to the suction. The injection slot should be located as close to the leading edge as possible, but should be located downstream of the suction peak. This is to make use of the adverse pressure gradient after the suction peak to enhance the wall jet mixing with the main flow[16]. In [9, 10], the injection slot size effect is studied experimentally. It is found that the smaller injection slot has higher stall AoA and hence high maximum lift. The energy expenditure of the airfoil with smaller injection slot is significantly less than that of the airfoil with large injection slot size. This indicates that there is a great potential to optimize the CFJ airfoil performance such as reducing the amount of jet mass flow with optimum configuration or pulsed jet, etc.

The coflow jet airfoil concept suggested by Zha el al. [8, 9] appears to have the following advantages: 1) Very effective to enhance lift and suppress separation; 2) Dramatically reduce drag and can achieve very high C_L/C_D at low AoA(cruise), and very high lift and drag at high AoA(take off and landing); 3) Significantly increase AoA operating range and stall margin; 4) Have small penalty to the propulsion system; 5) Can be applied to any airfoil, thick or thin; 6) Can be used for whole flying mission instead of only take off and landing; 7) Can be used for low and high speed aircraft; 8) Easy implementation with no moving parts;

The CFJ airfoil concept is new and hence many issues of the working mechanism need to be further studied. One question is: Compared with the CC airfoil which has no suction, will the streamwise suction of the CFJ airfoil hurt the airfoil performance? This question is based on the conception that a streamwise injection will generate a thrust due to its momentum and hence reduce the drag, a streamwise suction will do the opposite. However, any flow control process involved an injection must need a suction, which is the law of mass conservation, unless the jet is generated internally such as the rocket combustion. The question then becomes: where and how the suction occurs will be more beneficial, the suction occurring on the airfoil suction surface such as a CFJ airfoil (see Fig. 1) or the suction occurring on the engine such as a CC airfoil (see Fig.2)? To answer above question, a control volume analysis is given in [17]. The CFJ airfoil with both injection and suction is compared with the airfoil with injection only at one angle of attack in [17].

This purpose of this paper is to make a further effort to compare the CFJ airfoil with both injection and suction and the airfoil with injection only at the full range of AoA until the airfoils stall based on numerical simulations. This study has found that letting the suction occur on the airfoil suction surface such as the CFJ airfoil is more beneficial than letting the suction occur through the aircraft engine inlet. The CFJ airfoil with both injection and suction results in higher lift, higher stall margin, lower drag and lower energy expenditure.

3 Jet Reaction Forces

3.1 CFJ airfoil with both injection and suction

In [17], a control volume analysis gives the formulations to calculate the lift and drag contributed by the reaction forces generated by the injection and suction ducts. The CFJ airfoil integrated with a propulsion system can be illustrated as in Fig.1.

The drag of a CFJ airfoil is:

$$D = R'_x - F_{xcfj} \quad (1)$$

Or

$$D = \int_h^b \rho V_e (V_\infty - V_e) dy \quad (2)$$

Where R'_x is the drag from the airfoil surface integral of shear stress and pressure. F_{xcfj} is the drag due to the reaction forces generated by the injection and suction ducts and is:

$$\begin{aligned} F_{xcfj} &= (\dot{m}_{j1} u_{j1} + (p_{j1} A_{j1})_x) - \gamma (\dot{m}_{j2} u_{j2} + (p_{j2} A_{j2})_x) \\ &= (\dot{m}_j V_{j1} + p_{j1} A_{j1}) * \cos(\theta_1 - \alpha) - \gamma (\dot{m}_j V_{j2} + p_{j2} A_{j2}) * \cos(\theta_2 + \alpha) \end{aligned} \quad (3)$$

Where, γ is the suction coefficient. If $\gamma = 1$, the suction is on. If $\gamma = 0$, the suction is off and the co-flow jet has injection only. The θ is the angle between the slot surface and the line normal to the airfoil chord. For the CFJ0025-065-196 airfoil[9] studied in this paper, $\theta_1 = 25.86^\circ$, $\theta_2 = 14.31^\circ$, α is the angle of attack, V_j is the jet velocity, p_j is the jet static pressure, \dot{m}_j is the jet mass flow rate, A_j is the jet slot area.

For a CFJ airfoil, the wind tunnel measured drag is the actual drag that the aircraft will experience. This is different from an airfoil with injection only such as a circulation control airfoil[17, 18]. For an airfoil with injection only, the actual drag, or equivalent drag, is the drag measured in wind tunnel plus the drag due to the suction of the jet mass from the freestream, which includes the ram drag and captured area drag. The reason for the difference between a 2D CFJ airfoil and the airfoil with injection only is: for the 2D CFJ airfoil, the mass conservation is satisfied due to recirculating the jet; for the airfoil with injection only such as a circulation control airfoil, the 2D airfoil does not satisfy the mass conservation since there is no source for the jet injection.

The lift of a CFJ airfoil is:

$$L = R'_y - F_{y_{cfj}} \quad (4)$$

Where R'_y is the y-direction component of the surface pressure and shear stress integral, which is primarily induced by the circulation. $F_{y_{cfj}}$ is the jet ducts reaction force component in y-direction.

$$\begin{aligned} F_{y_{cfj}} &= (\dot{m}_{j1}v_{j1} + (p_{j1}A_{j1})_y) - \gamma(\dot{m}_{j2}v_{j2} + (p_{j2}A_{j2})_y) \\ &= (\dot{m}_jV_{j1} + p_{j1}A_{j1}) * \sin(\theta_1 - \alpha) + \gamma(\dot{m}_jV_{j2} + p_{j2}A_{j2}) * \sin(\theta_2 + \alpha) \end{aligned} \quad (5)$$

The CFD procedure to calculate the lift and are is: 1) calculate the surface integrals of the pressure and shear stress R'_x and R'_y ; 2) calculate the jet ducts reaction forces, $F_{x_{cfj}}$ and $F_{y_{cfj}}$; 3) calculate the total drag and lift based on Eqs. (1) and (4).

3.2 CFJ airfoil with injection only

Based on the control volume analysis given in [17], when an airfoil has injection jet only, the measured drag by the wind tunnel balance is:

$$\begin{aligned} D_{windtunnel} &= R'_x - (\dot{m}_ju_j + (p_jA_j)_x) = R'_x - (\dot{m}_jV_{j1} + p_{j1}A_{j1}) * \cos(\theta_1 - \alpha) \\ &= \int_h^b \rho V_e (V_\infty - V_e) dy - m_j V_\infty \end{aligned} \quad (6)$$

$$C_{D_{windtunnel}} = C_{D_{rake}} - C_\mu \frac{V_\infty}{V_j} \quad (7)$$

That is: for an airfoil with jet blowing only, the drag measured by the balance in a wind tunnel is equal to the drag calculated based on the wake rake measurement minus $m_j V_\infty$.

However, in reality, when the airfoil with jet blowing only is used in an aircraft, there must be an air flow source for the blowing. Usually, the engine sucks in the air from the freestream and injects on the wing surface as shown in Fig. 2. Drawing the air flow from the freestream will increase the drag of the system. The actual drag that the airfoil will experience, or the equivalent drag is:

$$\begin{aligned} C_{Dequiv} &= C_{D_{windtunnel}} + C_\mu \frac{V_{ei}}{V_j} + C_\mu \frac{V_{ei}}{V_j \gamma M_{ei}^2} \\ &= C_{D_{windtunnel}} + C_\mu \frac{V_{ei}}{V_j} \left(1 + \frac{1}{\gamma M_{ei}^2}\right) \end{aligned} \quad (8)$$

The 2nd term in Eq.(8) is the ram drag and the 3rd term is the captured area drag. Eq.(8) indicates that, when the Mach number at engine inlet is increased, the ram drag is also increased due to the higher velocity, and the captured area drag is decreased due to the reduced captured area for the jet. The captured area drag is significantly larger than the ram drag if the flow at engine inlet is subsonic. During a flight mission, the flow parameters at the engine inlet may or may be equal to the freestream parameters. For example, at the starting point to take off, the freestream velocity is zero, but the velocity at the engine inlet is far greater than zero to satisfy the engine mass flow requirement to generate the required thrust. During a flight mission, when the mass flow rate required by the engine is equal to the mass flow rate captured by the straight flow tube going into the engine inlet, the freestream flow parameters will be equal to the flow parameters at engine inlet. The drag increase for the airfoil with injection only due to the ram and captured area drag can be also considered as the loss of thrust[11].

If assume $V_{ei} = V_{\infty}$, based on Eq.(7), we have:

$$C_{Dequiv} = C_{Drake} + C_{\mu} \frac{V_{ei}}{V_j \gamma M_{ei}^2} \quad (9)$$

The lift for the airfoil with injection only is:

$$L = R'_y - (\dot{m}_{j1} v_{j1} + (p_{j1} A_{j1})_y) = R'_y - (\dot{m}_j V_{j1} + p_{j1} A_{j1}) * \sin(\theta_1 - \alpha) \quad (10)$$

The jet suction from the freestream has no component in y-direction. Hence the lift above is the same as the lift measured by the wind tunnel balance.

The equivalent drag formulation used in [18, 19] is different from the one given in [17]. The assumption used in [18, 19] is that the jet is taken from a large reservoir. As a reference, the formulation used in [18, 19] is given below:

$$C_{Dequiv} = C_{Dwindtunnel} + C_{\mu} \frac{V_{\infty}}{V_j} + C_{\mu} \frac{V_j}{2V_{\infty}} \quad (11)$$

Using Eq.(7),

$$C_{Dequiv} = C_{Drake} + C_{\mu} \frac{V_j}{2V_{\infty}} \quad (12)$$

4 Geometry

Fig.3 shows the baseline airfoil, NACA0025, the injection only CFJ airfoil, and the standard CFJ airfoil with both injection and suction. The NACA0025 airfoil was selected as the baseline airfoil due to its large thickness to facilitate implementation of co-flow jet, internal ducts, and instrumentation for wind tunnel tests[9, 10]. The chord length of the airfoil is 0.1527m and the span is 0.3m. The co-flow jet airfoils are named using the following convention: CFJ4dig-INJ-SUC, where 4dig is the same as NACA 4 digit convention, INJ is replaced by the percentage of the injection slot size to the chord length and SUC is replaced by the percentage of the suction slot size to the chord length. For example, the CFJ0025-065-196 airfoil has the injection slot height of 0.65% of the chord and the suction slot height of 1.96% of the chord. The new suction surface shape is a downward translation

of the portion of the original suction surface between the injection and suction slot. The injection and suction slot are located at 7.11% and 83.18% of the chord from the leading edge. The slot faces are normal to the suction surface to make the jet tangential to main flow.

The injection only CFJ airfoil has exactly the same injection slot geometry as the CFJ0025-065-196 airfoil. The suction surface is a vertical translation of the baseline NACA0025 airfoil suction surface. The chord length is 0.14729m and is slightly less than that of the baseline NACA0025 and CFJ0025-065-196 airfoil. Following this naming convention, the injection only CFJ airfoil is named as CFJ0025-065-000 airfoil.

5 CFD Solver

The Fluent CFD software is used in this research to calculate the 2D and 3D CFJ airfoil flows. The governing equations are the Reynolds averaged 3D compressible Navier-Stokes (RANS) equations. The pressure based second order upwind scheme is used to evaluate the inviscid flux and central differencing is used for the viscous terms. The $k - \epsilon$ turbulence model with integration to the wall and pressure gradient effect is employed. The y_1^+ is in the order of 1. The $k - \epsilon$ model is selected due to its capability of taking into account of turbulent boundary layer history effect by solving the complete transport equations of k and ϵ , and the $k - \epsilon$ model is more capable than algebraic models to predict the separated flows, which occur when the airfoil stalls at high AoA.

The full turbulent boundary layer assumption is used and is consistent with the tripped boundary layer in the experiments. Mesh refinement study is conducted for a few selected points to ensure that the solutions are mesh size independent. Since the CFD solutions are obtained from the steady state calculations based on RANS model, the unsteady details of the shear layer mixing entrainment and large coherent vortex structures are not able to be captured.

The total pressure and total temperature are given at the wind tunnel inlet as the boundary conditions. The static pressure at wind tunnel exit is iterated to make the wind tunnel inlet Mach number match the experimental value. The total pressure and total temperature are also given at the injection duct inlet as the boundary conditions. The injection total pressure is iterated to match the experimental momentum coefficient. The static pressure at the suction duct entrance is iterated to match the injection jet mass flow rate.

As mentioned above, several layers iterations are needed to achieve a converged CFJ airfoil solution at a certain AoA. The calculation is thus very CPU intensive, in particular for 3D cases. The 2D CFJ airfoil calculation is therefore very desirable. The control volume analysis in [17] provides the formulation to include the lift and drag generated by the jet ducts.

6 Results and Discussion

Fig. 4 is the zoomed mesh of the CFJ0025-065-000 airfoil. The mesh size is about 280k cells. The far-field boundary is 20 chord length away from the airfoil. The freestream Mach number is about 0.1 and the Reynolds number based on chord is 380k. The flow is assumed normal to the injection duct inlet. For the CFJ0025-065-196 airfoil, the suction duct is only simulated with an entrance opening since the flow inside the suction duct has little effect on the flow outside of the suction duct. Simulation of the injection duct gives a more realistic injection mixing effect when the jet enters into the mainflow.

The CFJ0025-065-196 airfoil has wind tunnel tests results given in [9, 10]. To compare the CFJ0025-065-000 airfoil with CFJ0025-065-196 airfoil, the same injection momentum coefficient obtained in the experiment is intended to be used. Figure 5 is the computed momentum coefficients compared with the experiment at different AoA. The deviation of the momentum coefficients is less than 5%.

Fig. 6 is the comparison of the lift coefficient for the CFJ0025-065-000 airfoil, CFJ0025-065-196 airfoil and the baseline NACA0025 airfoil. The experiment shows that the baseline airfoil stalls at AoA= 19°. The computed baseline airfoil lift coefficient agrees fairly well with the experiment, except that the stall AoA is about 3° higher. The computed lift coefficients of the CFJ airfoils include the jet reaction force effect determined by Eq.(4) and (10). Both CFJ0025-065-000 and CFJ0025-065-196 airfoil have higher lift coefficient and stall AoA than the baseline airfoil. For the CFJ0025-065-196 airfoil, the lift coefficient is under-predicted, in particular at high AoA. The computed lift coefficient shows that the CFJ0025-065-196 airfoil has higher lift than the CFJ0025-065-000 airfoil. The CFJ0025-065-000 airfoil stalls at AoA=39°. By the time that this paper is written, the CFJ0025-065-196 airfoil still has not stalled yet at AoA=43°, which means that the CFJ0025-065-196 airfoil has higher stall AoA than the CFJ0025-065-000 airfoil. Further calculation is in progress to determine the numerical stall AoA of the CFJ0025-065-196 airfoil.

Fig. 7 is the comparison of the drag coefficient for the CFJ0025-065-000, CFJ0025-065-196 airfoil and the baseline NACA0025 airfoil. The CFD slightly under-predicts the baseline airfoil drag coefficient when AoA ≤ 10°. The predicted drag coefficient remains flat at high AoA for the baseline airfoil, whereas the measured baseline airfoil drag coefficient increases at high AoA. The discrepancy of the baseline airfoil drag prediction is hence fairly large at high AoA.

The computed drag coefficients of CFJ0025-065-000 and CFJ0025-065-196 airfoil include the jet reaction force effect determined by Eq.(1) and (6). For the CFJ0025-065-196 airfoil, the measured drag is lower than that of the baseline airfoil. The computed drag of CFJ0025-065-196 airfoil shows the same trend, but is also under-predicted. At high AoA, the CFJ airfoil drag prediction is similar to the baseline case and is fairly flat, whereas the measured drag is increased. The predicted drag discrepancy of the CFJ0025-065-196 airfoil is hence particularly large at high AoA. This may be due to the inadequate turbulence mixing simulation by RANS model. The computed results indicate that the CFJ0025-065-000 airfoil (open square symbols) has lower 2D drag than the CFJ0025-065-000 airfoil (open circle symbols), in particular at high AoA.

The equivalent drag of the CFJ0025-065-000 airfoil is significantly higher than the drag of the baseline airfoil and the CFJ0025-065-196 airfoil by either Eq.(8) [17] or Eq.(11) [18]. The equivalent drag calculated based on Eq.(8) [17] is significantly higher than that determined by Eq.(11) [18]. For CFJ0025-065-196 airfoil, the equivalent drag is the same as the 2D drag and hence is significantly lower than that of the CFJ0025-065-000 airfoil. The lower drag means lower energy expenditure.

Figure 8 to 10 compare the computed wake profiles one chord downstream of the airfoil trailing edge between the CFJ0025-065-000 and CFJ0025-065-196 airfoil at AoA=10°, 20° and 30°. The CFJ0025-065-000 airfoil has deep velocity deficit. The CFJ0025-065-196 airfoil has reversed velocity up to AoA= 20°. The drag of CFJ0025-065-196 airfoil is determined by the wake profile as indicated by Eq.(2). The reversed velocity deficit means that the airfoil has negative drag, that is a thrust. The CFD under-predicts the drag since the measured drag is negative at AoA=0° and become positive when AoA is greater than 10°. The wake profile of CFJ0025-065-196 airfoil at AoA=30° is much shallower than that of the CFJ0025-065-000 airfoil as shown in Fig. 10. The only difference between these two airfoils is that the former has suction and the latter does not

have the suction. This means that the suction on the CFJ0025-065-196 airfoil significantly enhance the mixing and energy transfer between the jet and the main flow. Such higher mixing rate induces higher circulation and leading edge suction, which results in higher lift and lower drag.

Figure 11 and 12 are the Mach contours with streamlines of the CFJ0025-065-000 and CFJ0025-065-196 airfoil at $AoA=20^\circ$. They indicate again that the CFJ0025-065-000 airfoil has a large deep wake region with low momentum, whereas the CFJ0025-065-196 airfoil virtually has no wake. This is consistent as the wake profile given in Fig.9. The streamlines in the leading edge region show that the stagnation point of the CFJ0025-065-196 airfoil is more downstream than that of the CFJ0025-065-000 airfoil, which means that the CFJ0025-065-196 airfoil has higher circulation than the CFJ0025-065-000 airfoil.

Figure 13 to 15 are the surface isentropic Mach number distributions of the CFJ0025-065-000 and CFJ0025-065-196 airfoil at $AoA=10^\circ$, 20° and 30° . They show that the CFJ0025-065-196 airfoil always has higher overall loading (lift), higher leading edge suction peak Mach number, and more downstream stagnation point location. The stronger leading edge suction results in a resultant pressure force pushing forward, which either generates a thrust or reduces the overall drag.

7 Conclusions

The CFJ airfoil with injection only (CFJ0025-065-000 airfoil) is compared with the CFJ airfoil with both injection and suction (CFJ0025-065-196 airfoil) with the similar injection momentum coefficient. The CFD simulations indicates that the suction of the CFJ0025-065-196 airfoil significantly enhance the mixing and energy transfer between the jet and main flow, which results in higher circulation, higher lift, higher stall AoA , lower drag, and lower energy expenditure. The equivalent drag of the airfoil with injection only is significantly higher than that of the CFJ airfoil with both injection and suction. Since any airfoil with a jet injection needs to have a jet suction to satisfy the mass conservation law, this study indicates that the suction occurring on the suction surface such as the CFJ airfoil is more beneficial than drawing the jet mass flow from the aircraft engine.

References

- [1] W. L. I. Sellers, B. A. Singer, and L. D. Leavitt, "Aerodynamics for Revolutionary Air Vehicles." AIAA 2004-3785, June 2003.
- [2] M. Gad-el Hak, "Flow Control: The Future ," *Journal of Aircraft*, vol. 38, pp. 402–418, 2001.
- [3] M. Gad-el Hak, *Flow Control, Passive, Active, and Reactive Flow Management*. Cambridge University Press, 2000.
- [4] S. Anders, W. L. Sellers, and A. Washburn, "Active Flow Control Activities at NASA Langley." AIAA 2004-2623, June 2004.
- [5] C. P. Tilmann, R. L. Kimmel, G. Addington, and J. H. Myatt, "Flow Control Research and Application at the AFRL's Air Vehicles Directorate." AIAA 2004-2622, June 2004.
- [6] D. Miller, , and G. Addington, "Aerodynamic Flowfield Control Technologies for Highly Integrated Airframe Propulsion Flowpaths." AIAA 2004-2625, June 2004.

- [7] V. Kibens and W. W. Bower, “An Overview of Active Flow Control Applications at The Boeing Company.” AIAA 2004-2624, June 2004.
- [8] G.-C. Zha and C. Paxton, “A Novel Airfoil Circulation Augment Flow Control Method Using Co-Flow Jet.” NASA/CP-2005-213509, June 2005; AIAA Paper 2004-2208, June 2004.
- [9] G.-C. Zha, B. Carroll, C. Paxton, A. Conley, and A. Wells, “High Performance Airfoil with Co-Flow Jet Flow Control.” AIAA-Paper-2005-1260, Jan. 2005, submitted for publication in AIAA Journal.
- [10] G.-C. Zha, C. Paxton, A. Conley, A. Wells, and B. Carroll, “Effect of Injection Slot Size on High Performance Co-Flow Jet Airfoil.” to appear in AIAA Journal of Aircraft, 2006.
- [11] G.-C. Zha and D. C. Paxton, “A Novel Flow Control Method for Airfoil Performance Enhancement Using Co-Flow Jet.” *Applications of Circulation Control Technologies*, Progress in Astronautics and Aeronautics, AIAA Book Series, Editors: Joslin, R. D. and Jones, G.S., to be published in 2006.
- [12] R. J. Englar, “Circulation Control for High Lift and Drag Generation on STOL Aircraft,” *Journal of Aircraft*, vol. 12, pp. 457–463, 1975.
- [13] R. J. Englar, L. A. Trobaugh, and R. Hemmersly, “STOL Potential of the Circulation Control Wing for High-Performance Aircraft,” *Journal of Aircraft*, vol. 14, pp. 175–181, 1978.
- [14] Y. Liu, L. N. Sankar, R. J. Englar, K. K. Ahuja, and R. Gaeta, “Computational Evaluation of the Steady and Pulsed Jet Effects on the Performance of a Circulation Control Wing Section.” AIAA Paper 2004-0056, 42nd AIAA Aerospace Sciences Meeting and Exhibit, Reno, Nevada 5 - 8 Jan 2004.
- [15] I. Wygnanski, “The Variables Affecting The Control Separation by Periodic Excitation.” AIAA 2004-2625, June 2004.
- [16] E. M. Greitzer, C. S. Tan, and M. B. Graf, *Internal Flow*. Cambridge University Press, 2004.
- [17] G.-C. Zha and W. Gao, “Analysis of Jet Effects on Co-Flow Jet Airfoil Performance with Integrated Propulsion System.” AIAA Paper 2006-0102, 2006.
- [18] G. S. Jones, “Pneumatic Flap Performance for a 2D Circulation Control Airfoil, Steady & Pulsed.” NASA/CP-2005-213509, June 2005, and *Applications of Circulation Control Technologies*, Progress in Astronautics and Aeronautics, AIAA Book Series, Editors: Joslin, R. D. and Jones, G.S., to be published in 2006.
- [19] M. Wilson and C. von Kerczek, “An Inventory of Some Force Procedure for Use in Marine Vehicle Control.” DTNSRDC-791097, Nov, 1979.

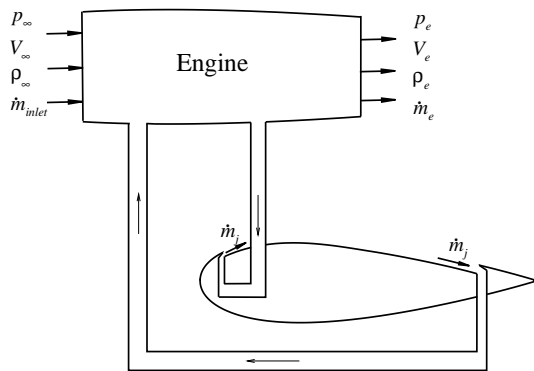


Figure 1: Sketch of a CFJ airfoil integrated with a propulsion system.

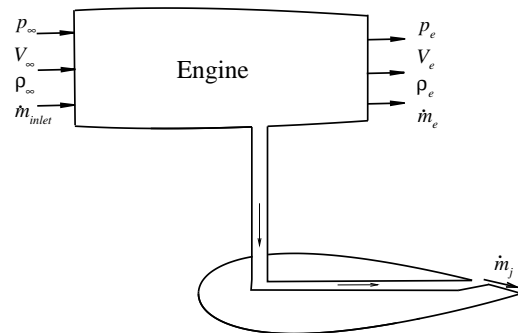


Figure 2: Sketch of an injection airfoil integrated with a propulsion system.

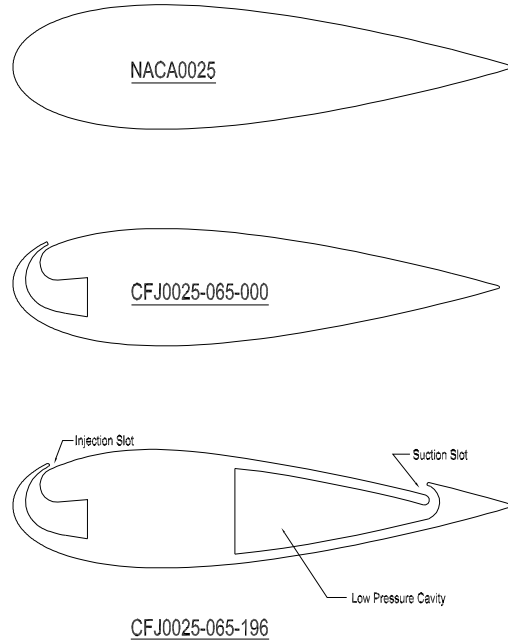


Figure 3: Airfoil section of the baseline airfoil NACA0025, injection only CFJ airfoil, and regular CFJ airfoil.

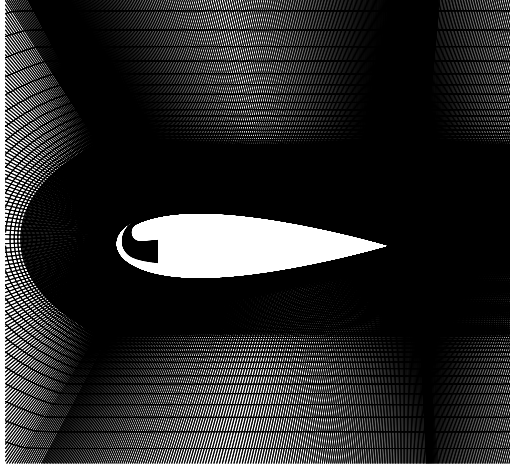


Figure 4: The zoomed mesh around the CFJ0025-065-000 airfoil.

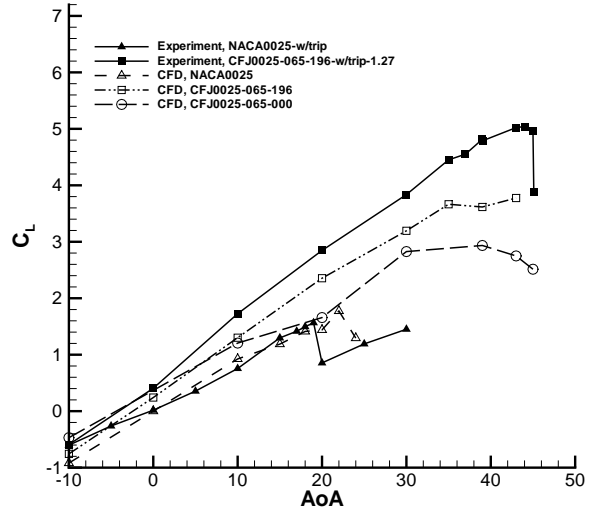


Figure 6: Comparison of the computed lift coefficient with experiment.

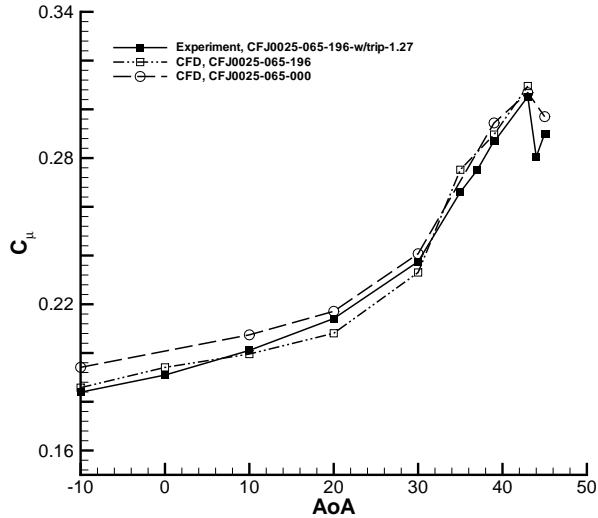


Figure 5: Comparison of computed momentum coefficient with experiment.

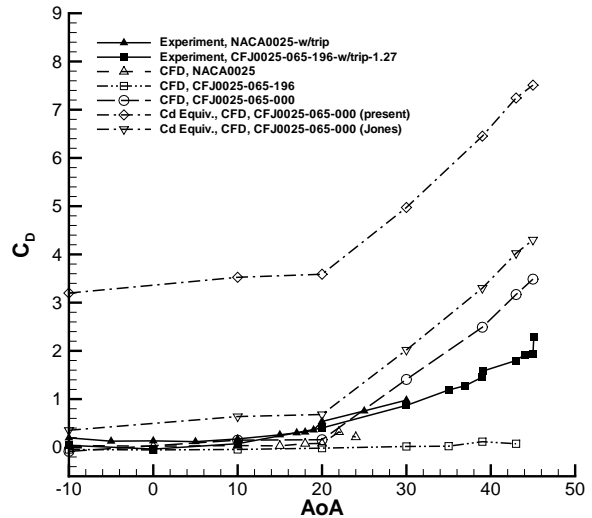


Figure 7: Comparison of the computed drag coefficient with experiment.

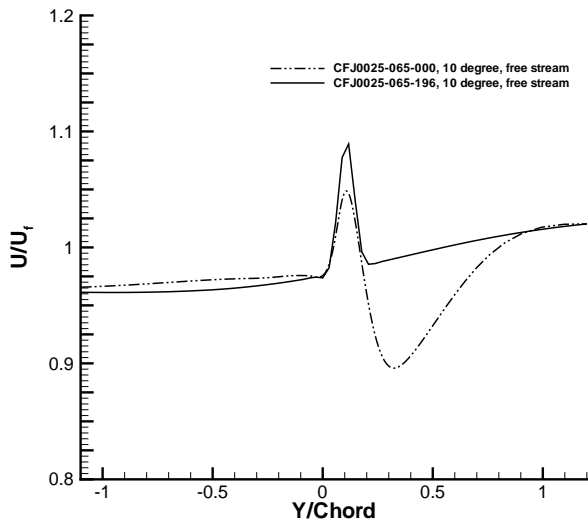


Figure 8: Comparison of the computed wake profile at $AoA=10^\circ$.

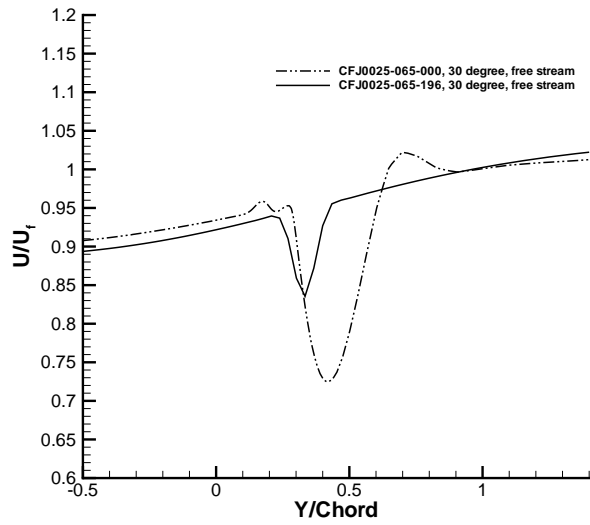


Figure 10: Comparison of the computed wake profile at $AoA=30^\circ$.

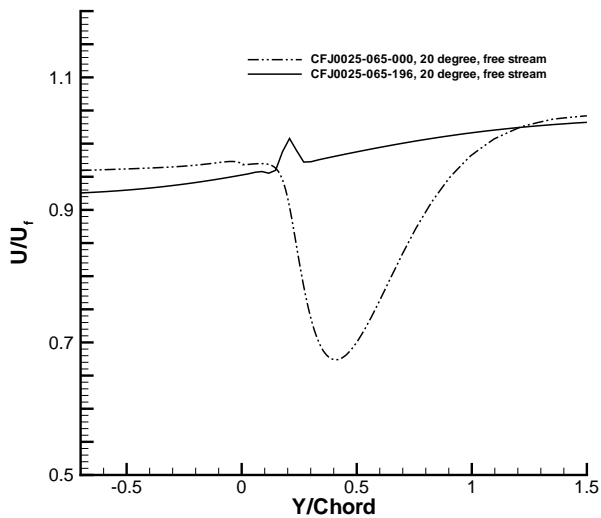


Figure 9: Comparison of the computed wake profile at $AoA=20^\circ$.

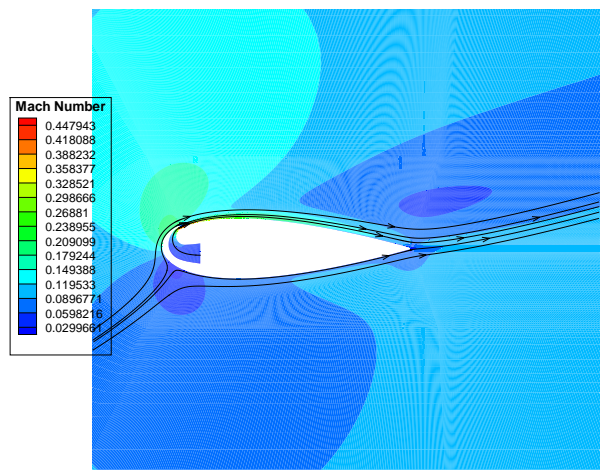


Figure 11: Mach contours with streamlines of the CFJ0025-065-000 airfoil at $AoA=20^\circ$.

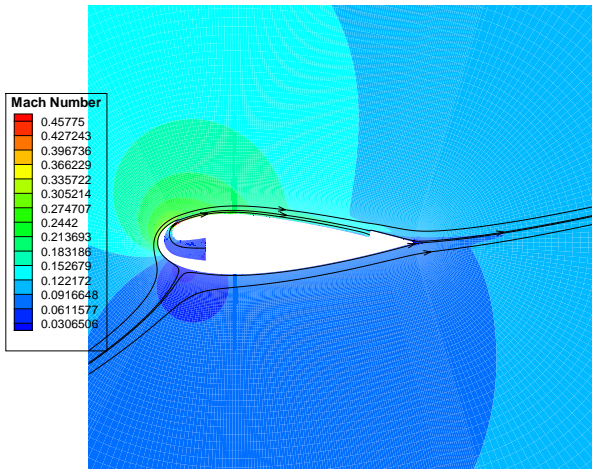


Figure 12: Mach contours with streamlines of the CFJ0025-065-196 airfoil at $AoA=20^\circ$.

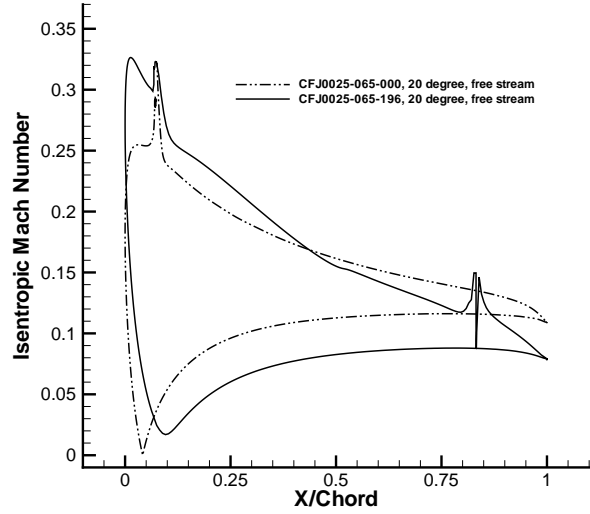


Figure 14: Comparison of the computed surface isentropic Mach number distribution at $AoA=20^\circ$.

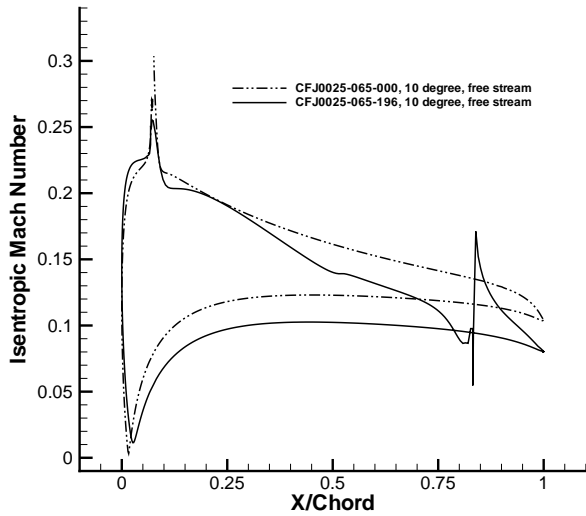


Figure 13: Comparison of the computed surface isentropic Mach number distribution at $AoA=10^\circ$.

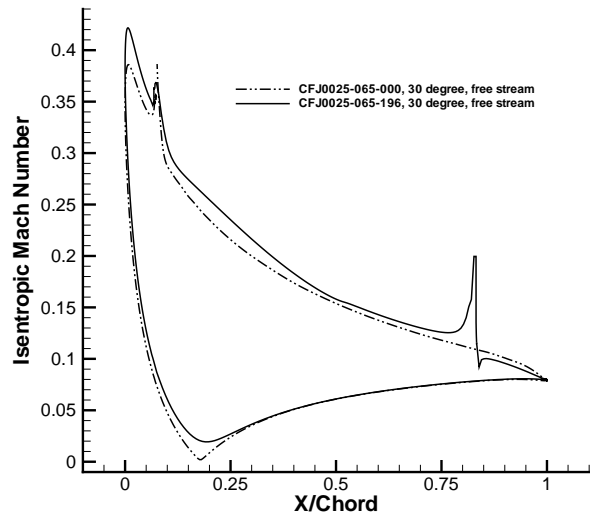


Figure 15: Comparison of the computed surface isentropic Mach number distribution at $AoA=30^\circ$.